Anhydrous Methanol and Ethanol Dehydrogenation at Cu(111) Step Edges

Robert A. Hoyt,[†] Matthew M. Montemore,[‡,¶] E. Charles H. Sykes,[§] and Efthimios Kaxiras[*,†,¶]

Department of Physics, Harvard University, Cambridge, MA 02138, USA, Department of Chemistry and Chemical Biology, Harvard University, Cambridge, MA 02138, John A. Paulson School of Engineering and Applied Sciences, Harvard University, Cambridge, Massachusetts 02138, USA, and Department of Chemistry, Tufts University, Medford, Massachusetts 02155, USA

E-mail: kaxiras@physics.harvard.edu

[*]To whom correspondence should be addressed
[†]Harvard University Department of Physics
[‡]Harvard University Department of Chemistry and Chemical Biology
[¶]Harvard University John A. Paulson School of Engineering and Applied Sciences
[§]Tufts University Department of Chemistry

Abstract

Oxidative methanol dehydrogenation is a major industrial reaction with global formaldehyde production exceeding 30 million tonnes per year. Unfortunately, oxidative dehydrogenation produces water-aldehyde mixtures that require subsequent distillation. Anhydrous alcohol dehydrogenation is a promising alternative that produces H_2 instead of water. Pursuant to recent experimental work showing that highly stepped Cu(111) surfaces exhibit anhydrous dehydrogenation activity, we present first-principles density functional theory calculations for methanol and ethanol dehydrogenation at Cu(111) step edges to provide an atomistic understanding of the catalytic mechanism; these sites stabilize all intermediates while reducing activation energies. We find that van der Waals contributions to the energy account for more than 50% of adsorption energies, and their inclusion is essential in achieving good agreement with experimental desorption temperatures. Furthermore, vibrational zero-point energy corrections significantly reduce the activation energy for all reaction steps considered here. Hydrogen bonding among ethanol intermediates at step edges is weakened by geometric frustration. These insights lead us to propose several suggestions for further research on undercoordinated Cu sites as anhydrous alcohol dehydrogenation catalysts.

Introduction

Improving the performance of industrial catalysts requires increasing their activity and selectivity while maintaining long catalyst lifetime. Alcohol dehydrogenation on heterogeneous catalysts is the most significant industrial pathway for formaldehyde production,[1,2] with global production exceeding 30 million tonnes per year. Current catalysts, either based on silver or oxides of iron, molybdenum and vanadium[3] require oxygen to facilitate alcohol oxidation and therefore produce water as a byproduct. Separating formaldehyde and unreacted methanol from water requires energy-intensive absorber and vacuum distillation stages.[2,4] If catalysts were able to function in the absence of oxygen, industrially valuable H_2 would

be produced instead of water. Such catalysts are not commercially available yet, but further improvements to promising candidates may lead to better prospects. Cu is particularly promising due to its low cost, high selectivity,[1] and long catalyst lifetimes.

Substantial experimental work has addressed alcohol dehydrogenation on Cu surfaces. Much of this research has focused on oxidative dehydrogenation over single-crystal surfaces, starting with Cu(110)[5] and Cu(111).[6] The consensus is that O–H bond breaking occurs at low temperatures to produce stable alkoxy intermediates, followed by reaction rate-limited aldehyde desorption at higher temperatures. Hydrogen adatoms generated from breaking methoxy C–H bonds can also lead to methoxy hydrogenation and reaction rate-limited methanol desorption.[5] Detailed adsorbate-surface distance measurements for methanol and methoxy intermediates at low temperature have been made with X-ray standing wave adsorption experiments.[7] More detailed results for adsorbate geometry and induced surface relaxation are also available for methoxy on the Cu(111) surface.[8] Under ultra-high vacuum (UHV) conditions, defect-free Cu single-crystal surfaces (except Cu(210)[9]) are inert toward alkoxy dehydrogenation[5,10] such that a co-catalyst is required to facilitate C–H bond breaking. Early studies employed adsorbed oxygen atoms as the co-catalyst and produced water as a byproduct.[5,6,10] Later it was demonstrated that water itself serves as a co-catalyst for methoxy dehydrogenation to formaldehyde and H_2[11,12] through water-alcohol and water-alkoxy hydrogen bonding. In an effort to remove water from the reaction cycle entirely, more recent work on Cu(111) surfaces has demonstrated that surface defects, either isolated dopant metal atoms[12,13] or step edges,[14] can supplant water as an effective co-catalyst to facilitate anhydrous alcohol dehydrogenation. These defect studies also observed O–H bond breaking at low temperatures followed by C–H bond breaking at higher temperatures.

Several previous theoretical studies based on density functional theory (DFT) examined a variety of methanol dehydrogenation intermediates at flat and stepped Cu(111) surfaces. Greeley and Mavrikakis[15] found that methanol adsorbs to Cu top sites through its O atom, while formaldehyde adsorbs flat on Cu(111). They also find the same reaction mechanism as

observed in experiments. A related study on 22-atom Cu(111)-terminated clusters[16] reported qualitatively similar energetics, but found that methanol adsorbs at top sites through the alcohol H atom, and that formaldehyde adsorbs perpendicular to the surface though weak O–Cu and H–Cu bonds. Methanol dehydrogenation intermediates have also been studied in the context of methanol synthesis with DFT and van der Waals (vdW) corrections on the stepped Cu(211) surface.[17,18] Step edges stabilized all adsorbates and improved reactivity, while vdW interactions were significant for higher molecular weight adsorbates, particularly those derived from CO_2 rather than CO. While Cu(211) surfaces expose (100) steps, there also exist (111) steps, as discussed below. The (111) step has been studied with DFT for formaldehyde steam reforming using the Cu(221) surface,[19] where formaldehyde was found to adsorb above and parallel to the step edge.

The corresponding ethanol dehydrogenation pathway and its intermediates have been studied as well. A study of ethyl acetate synthesis on Cu(111) surfaces[20] found that ethanol adsorbs to the terrace through its alcohol H atom, while another study of ethanol adsorption found that it adsorbs to Cu(111) surfaces through its O atom instead.[21] Further work on CO hydrogenation to ethanol on Cu(211) surfaces found that all intermediates besides H are more stable at step edges,[22] and that H is most stable at three-fold hollow sites immediately below the step edge, while an earlier study[19] found that H is most stable at three-fold hollow sites immediately above the step edge. Although the predicted reaction mechanism for alcohol dehydrogenation agrees with experimental results, there is significant disagreement regarding adsorption geometries for alcohols and aldehydes.

To address the current lack of direct comparison between methanol and ethanol and between both Cu(111) step edges, as well as the lingering discrepancies among existing computational studies, we report here the adsorption geometries and energies for all key methanol and ethanol dehydrogenation intermediates on the Cu(111) terrace and its step edges. We take into account vdW interactions for all adsorbates and transition states as they have been shown to qualitatively alter adsorption energies and geometries for dehydrogenation

intermediates on Cu(111) surfaces[18,21] and other organic molecules on Au(111) and (100) surfaces.[23] Furthermore, while alcohol-alcohol hydrogen bond energies are significant in the gas phase[24] and on transition metal surfaces,[11,12,25,26] hydrogen bonding behavior has not been studied at Cu(111) step edges. We also include vibrational zero point energy (ZPE) corrections for all intermediates to provide a more realistic description.

Our theoretical comparison between methanol and ethanol can help identify trends that extend toward larger alcohols like n-propanol, and the difference in behavior at step edges versus on the Cu(111) terrace can reveal how local surface structure contributes to adsorbate stability and affects reaction rates. These detailed calculations elucidate the importance of step edges and contribute to a better understanding of catalyst design principles.

Computational Details

DFT and MD Parameters

Density functional theory (DFT) calculations were performed using VASP version 5.4.2[27–30] with the exchange-correlation functional of Perdew, Burke, and Ernzerhoff (PBE).[31,32] To achieve precisions of 0.01 eV for minimum-energy geometries we use plane wave cutoffs of 400 eV and relax geometries until the maximum force component is less than 0.01 eV/Å in magnitude using the FIRE method[33] from the VASP Transition State Tools (VTST) package. The Cu(111) surface is modeled with a 3×3 supercell, while the (111) and (100) step edges are modeled using three-atom-wide supercells of the (553) and (533) surfaces, respectively. All unit cells contain six layers in the (111) direction, with the bottom two layers fixed in their bulk positions and with a bulk-optimized lattice constant of 3.547 Å. To minimize interactions between periodic slab images we ensure that at least 10 Å of vacuum separates atoms in adjacent slabs, including any adsorbates, and we apply dipole energy corrections perpendicular to the slab. Monkhorst-Pack k-point meshes[34] are selected to achieve similar sampling densities across all three surfaces. With the convention $\vec{A}_i \cdot \vec{b}_j \equiv \delta_{ij}$ for lattice

vector $\vec{A}_i$ and reciprocal lattice vector $\vec{b}_j$, convergence is obtained using $m_i = |\vec{b}_i| \cdot 50$ Å points along lattice vector $\vec{A}_i$, rounding m_i to the nearest integer. This yields an 8×8 grid for the (111) surface, a 7×5 grid for the (111) step, and a 7×6 grid for the (100) step. For inter-adsorbate interactions, 4×4 Cu(111) supercells and four-atom-wide step surfaces were used with the same k-point density and otherwise-identical settings. Gas phase calculations use cubic unit cells with a side length of 30 Å. Molecular dynamics simulations use four total layers, plane wave cutoffs of 300 eV and $m_i = |\vec{b}_i| \cdot 35$ Å. These reduced values preserve most adsorption energies within 0.05 eV and yield very similar adsorbate geometries relative to the converged parameters. All energies include zero-point vibrational energy (ZPE) corrections, using 0.005 Å centered differences, and vdW corrections calculated with the Tkatchenko-Scheffler (TS) method.[35] All transition state geometries and energies are obtained using the dimer method,[36,37] as implemented in VTST, which improves the standard VASP version by rotating the dimer regardless of curvature to avoid pathological trajectories. Searches are initiated from several rotations and translations of the lowest-energy hydrogenated precursor with the cleaved O–H or C–H bond pre-stretched to approximately 1.3 Å to reduce its curvature. Dimer geometries are optimized using conjugate gradient minimization until the largest force is less than 0.02 eV/Å in magnitude. Reactant and product geometries are determined by displacing each transition state by ±0.25 Å along the unstable mode, then relaxing to the nearest local minimum using the conjugate gradient method. Finally, molecular dynamics (MD) simulations used a time step of 1 fs and a Nose-Hoover thermostat set to 150 K.

Structures and Energetics

The Cu(111) surface has two low index step facets as illustrated in Figure 1, with (111) or (100) orientations. The nomenclature of these step types is somewhat inconsistent in the literature; here we follow the convention used in studies of vicinal surfaces.[38] We refer to undercoordinated atoms at step edges as "step atoms," and to the bridge sites between them

"step bridges." Step atoms at both step edges are 7-fold coordinated and have identical radial distribution functions. The (111) and (100) step edges meet at 60° angles to form kink sites with either 6-fold coordination (lower left in Figure 1) or 8-fold coordination (upper right in Figure 1). Although these kinks most likely have different reactivities, we did not consider them in detail since scanning tunneling microscopy (STM) images show that adsorbates are found along the entirety of step edges. Preliminary calculations also show that adsorption energies at 6-fold-coordinated kink sites are stronger, but their O–H transition states have higher energies so they are predicted to be less reactive. Both step types are experimentally stable and similarly prevalent on the Cu(111) surface throughout the alcohol dehydrogenation reactions and above 400 K. Furthermore, while adatom and vacancy defects at step edges are also possible, we calculate that the formation energy of an adjacent adatom-vacancy pair is significantly endothermic relative to clean step edges: 0.55 eV for the (111) step, and 0.65 eV for the (100) step. Adatoms and vacancies increase alcohol adsorption energies by about 0.1 eV compared to clean steps so adsorbates cannot stabilize these adatom-vacancy pairs. O–H transition states also have higher energies on adatoms and defects than on clean step edges. As a result we did not consider such defects in detail.

Adsorption energies are significantly increased by vdW interactions, especially for the larger ethanol dehydrogenation intermediates where the extra CH_2 subunit typically contributes an additional 0.18 eV to adsorption energies. Table 1 shows the vdW contribution to alcohol and aldehyde desorption energies, defined as the fraction f_{vdW} of the total adsorption energy due to the TS vdW correction

$$f_{\mathrm{vdW}}(A) = \left(E_{\mathrm{TS}}(A/X) - E_{\mathrm{TS}}(A) - E_{\mathrm{TS}}(X)\right)/E_{\mathrm{des}} \tag{1}$$

where E_{TS} is the TS vdW contribution to the PBE+vdW energy for intermediate A adsorbed to surface X or in the gas phase, and E_{des} is the PBE+vdW desorption energy. All values

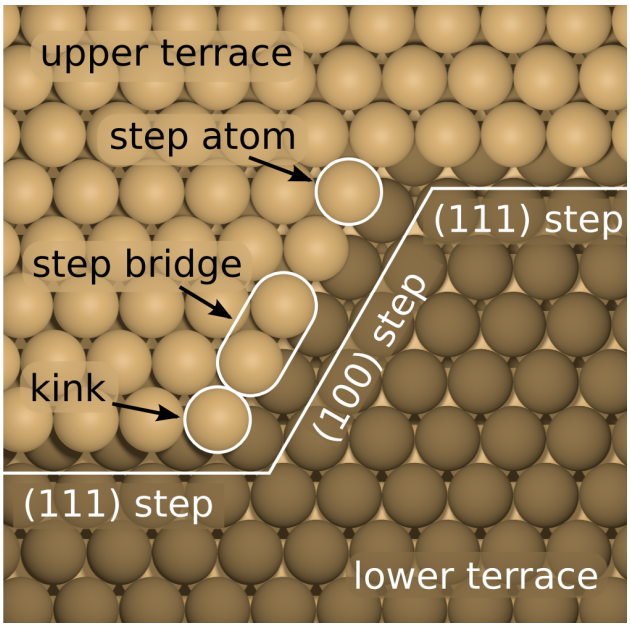

Figure 1: Primitive step features on the Cu(111) terrace. Cu atoms in the upper terrace are shaded light tan, while Cu atoms in the lower terrace are shaded dark tan.

are taken from the same PBE+vdW calculation. TS vdW corrections account for at least 54% of desorption energies at step edges, and at least 79% on the flat Cu(111) terrace. This is largely due to variations in the PBE contributions since the TS vdW corrections for each adsorbate are similar across all three sites. f_{vdW} exceeds 100% for aldehydes on the terrace; aldehyde-surface vdW interactions are so dominant they result in geometries with a negative PBE contribution. Undercoordinated step atom and bridge sites provide stronger adsorbate-Cu interactions and hence reduce the relative contributions of vdW interactions at step edges. Our binding energy and f_{vdW} values for ethanol on the Cu(111) surface are in reasonable agreement with previous results[21] using the similar D3 vdW correction scheme.[39] For methanol and formaldehyde we obtain significantly larger adsorption energies for the same adsorption geometries reported by Greeley and Mavrikakis[15] without vdW corrections. Similar increases in stability due to vdW corrections are also seen in previous work on Cu(110),[40] though with a smaller typical trend of 0.14 eV/CH_2 due to the lower atomic density at the Cu(110) surface.

In addition to increasing adsorbate stability, vdW contributions also affect adsorption

Table 1: Percent Contribution $f_{\mathbf{vdW}}$ of TS vdW Corrections to PBE+vdW Desorption Energies

Surface	MeOH	EtOH	CH_2O	CH_3CHO
(111) step	54	62	60	58
(100) step	61	66	53	64
terrace	79	87	111	111

geometries. The TS vdW corrections are exclusively attractive and therefore favor smaller adsorbate-surface distances. Previous comparisons of the PBE and PBE+vdW geometries of ethanol on Cu(111)[21] using D3 vdW corrections found that the C–C bond is approximately perpendicular to the surface with PBE alone, but is nearly parallel to the surface with PBE+vdW. Similarly, our alcohol adsorption geometries on the Cu(111) terrace feature slightly shorter adsorbate-Cu distances than previous methanol geometries with O–Cu bonding,[15] and much shorter than previous methanol[16] and ethanol[20] geometries with H–Cu bonding. The latter H–Cu adsorption geometries are unstable with PBE+vdW and relax to the O–Cu geometry. Force components were generally less than 0.1 eV/Å during the relaxation from H–Cu bonding to O–Cu bonding, demonstrating the importance of using stringent force criteria when working with weakly bound adsorbates. Adsorption geometries for aldehydes are similarly affected. Several previous studies without vdW corrections found that formaldehyde[16,41] and acetaldehyde[42] adsorb perpendicular to the surface with relatively large adsorbate-Cu distances, although flat formaldehyde adsorption geometries were only 0.02 eV less stable.[41] In contrast, perpendicular aldehyde geometries are unstable in PBE+vdW calculations and relax to lie flat on the terrace. Adsorption at step edges is similarly affected. Previous ethanol and acetaldehyde geometries at (100) steps[22] exhibited large angles between the C–C bond axis and the the upper terrace without vdW corrections, while the PBE+vdW geometries have C–C bonds parallel to the lower terrace. Similarly, vdW corrections reduced adsorbate-surface distances for alcohol dehydrogenation intermediates on Cu(110) surfaces as well.[40]

Another effect of vdW corrections is a reduction in the bulk-optimized lattice constant.

Our PBE+vdW calculations yield a lattice constant of 3.55 Å, 1.9% lower than the experimental value of 3.615 Å. Conversely, GGA-only calculations tend to overestimate lattice constants.[43] The PW91 functional predicts 3.66 Å for Cu,[15] and PBE predicts 3.67 Å.[44] Compared to the latter PBE-only value, the PBE+vdW value is equivalent to a 3.3% isotropic compression of the Cu lattice and should therefore affect its electronic and catalytic properties. For example, Greeley and Mavrikakis previously investigated the impact of a 4% lateral expansion on methanol dehydrogenation[15] on Cu(111) and found that expansion reduced the C–H activation energy by 0.06 eV and increased the stability of the methoxy intermediate by 0.18 eV. Similar effects are anticipated in the present study.

Table 2: Contribution of Zero-Point Vibrational Energy to Desorption and Activation Energies in eV

		Desorption Energy		Activation Energy	
Type	Site	Alcohol	Aldehyde	O–H	C–H
MeOH	(111) step	0.03	0.04	−0.21	−0.20
	(100) step	0.04	0.04	−0.21	−0.20
	terrace	0.04	0.01	−0.22	−0.21
EtOH	(111) step	−0.06	0.03	−0.22	−0.18
	(100) step	−0.06	0.03	−0.21	−0.22
	terrace	−0.06	0.03	−0.22	−0.23

Zero-point vibrational energy can significantly alter potential energy landscapes, especially for activation energies of bonds with high vibrational frequencies. O–H and C–H bonds have typical frequencies around 3000 cm^{-1} and therefore contribute $\hbar\omega/2 \sim 0.2$ eV. Thus, ZPE corrections are expected to be significant in these cases since cleaved bonds do not contribute to transition state ZPE corrections. For adsorbates, ZPE corrections can still be significant since molecular normal modes may change as a result of adsorbate-surface interactions. We therefore calculated ZPE corrections for all reaction intermediates and gas phase species. Table 2 shows the resulting ZPE corrections to the PBE+TS desorption and activation energies for alcohols and aldehydes. ZPE corrections are small for desorption energies, where adsorbate-surface interactions are too weak to significantly alter molecular normal modes. The total correction is at most 10% across all 12 adsorbate-site combina-

tions. On the other hand, ZPE corrections reduce activation energies by about 0.21 eV for all dehydrogenation reactions. This value is similar to the one predicted by the vibrational frequency of bonds which is approximately 3000 cm^{-1}. Comparing the stable normal modes of reactant and transition state geometries reveals no other significant differences for each reaction. Neglecting the approximately 0.21 eV ZPE corrections for bonds would therefore increase activation energies by up to 40% at step edges.

Dehydrogenation Intermediates

Steps increase the stability of all intermediates on the Cu(111) surface. Minimum-energy adsorption geometries at each site are shown in Figure 2 and their O–Cu bond lengths are shown in Table 3. Although both steps involve similar geometries for each intermediate, the reduced 7-fold coordination of step atoms leads to qualitatively different adsorption geometries compared to the flat Cu(111) terrace. All adsorbate-Cu bonds involve the O atom on all three surfaces, although the O–Cu coordination changes throughout the dehydrogenation process. A major finding is the similarity in adsorption and reactivity between methanol and ethanol intermediates. Both alcohols and their corresponding alkoxys have the same O–Cu coordination and very similar O–Cu bond lengths, as well as similar orientations relative to the surface. The corresponding aldehydes have weak preferences for different O–Cu coordinations, where formaldehyde prefers step bridges and acetaldehyde prefers step atoms.

Table 3: O–Cu Bond Distances for Minimum-Energy Adsorbate Geometries

Adsorbate	terrace	(111) step	(100) step
MeOH	2.23	2.17	2.22
EtOH	2.32	2.14	2.17
MeO	2.03	1.95	1.95
EtO	2.02	1.95	1.95
CH_2O	$2.99^{\perp}$	2.08	2.12
CH_3CHO	$3.06^{\perp}$	2.07	2.07

All distances are in Å.

$^{\perp}$ Distance from O atom to the Cu(111) surface plane

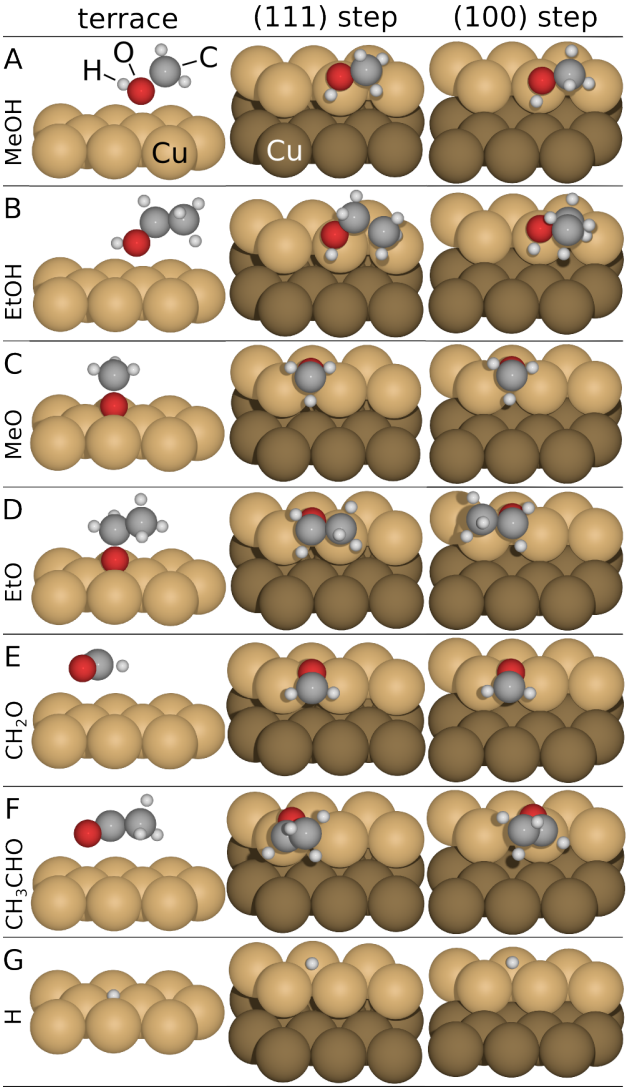

Figure 2: Minimum-energy adsorption geometries for isolated methanol and ethanol dehydrogenation intermediates. Cu atom colors indicate their position relative to the step: light tan for the upper terrace, and dark tan for the lower terrace.

Alcohols

Methanol and ethanol prefer dative O–Cu bonding through one of the oxygen lone pairs to top sites on every surface facet. As shown in rows A and B of Figure 2, methanol and ethanol have similar geometries and adsorb through binding to the O atom. Ethanol is more strongly bound on average by -0.18 eV, due to vdW interactions between its additional CH_2 subunit and the Cu surface. At steps, adsorption is significantly stronger at the undercoordinated step atoms. This yields shorter O–Cu distances at step sites, 2.14 to 2.24 Å, versus the terrace values of 2.30 Å for methanol and 2.32 Å for ethanol. Since the O-bonded Cu atom relaxes somewhat toward the alcohol, the average vertical distance between the O atom and the Cu(111) surface layer is slightly larger, 2.39 Å, for both alcohols, in fair agreement with the experimental value of 2.69 ± 0.19 Å for methanol.[7] Alcohol adsorption energies vary by at most 0.04 eV between the (111) and (100) step edges for both alcohols, indicating negligible preference for either step edge. Alcohols on the terrace feature O–H bonds approximately parallel to the surface and O–C bonds oriented at angles 36-37° from the surface. Alcohol geometries at steps have O–H bonds approximately perpendicular to the step edge and all carbon atoms are suspended over the lower terrace. The internal coordinates of adsorbed molecules are nearly identical to their gas phase values for all alcohol and step combinations. The only exception is ethanol in specific conformers. In the gas phase, there is negligible preference for trans over gauche (< 0.01 eV difference in energy). On the terrace, the preference is more significant and the trans conformer is more stable than the gauche conformer by 0.06 eV. In contrast, trans geometries are unstable at step edges and relax to the gauche conformer.

Alkoxys

Alkoxys have significantly different adsorption geometries on the terrace and steps as shown in rows C and D of Figure 2. Alkoxys on the terrace prefer fcc hollow sites, forming three O–Cu bonds of length 2.03 Å, and feature an O–C bond nearly perpendicular to the surface.

We find that the O atom in methoxy and ethoxy both have average vertical distances from the Cu(111) surface layer of 1.39 Å, in good agreement with a previous experimental value of 1.31 ± 0.06 Å,[7] and this previous study determined that methoxy adsorbs to both fcc and hcp hollow sites with negligible preference between the two. Earlier photoelectron diffraction experiments[8] found a similar average vertical distance of 1.32 ± 0.05 Å from the methoxy O atom to its three nearest Cu neighbors, which agrees well with our value of 1.35 Å for both methoxy and ethoxy. Moreover, the latter study found that the methoxy C–O bond is perpendicular to the surface with a length of $1.42^{+0.10}_{-0.03}$ Å, in excellent agreement with the minimum-energy orientation and C–O bond length of 1.42 Å. In contrast to the terrace, alkoxys at step sites occupy undercoordinated bridge sites, with the O–C bond perpendicular to the step direction and nearly coplanar with the lower terrace. Alkoxys at steps exhibit an additional preference for a methyl C–H bond directed toward the lower terrace with an energy gain of 0.03 eV. In contrast to the alcohols, the (100) step binds alkoxys more strongly than the (111) step, by 0.06 eV for methoxy and 0.02 eV for ethoxy.

Aldehydes

Minimum-energy aldehyde adsorption geometries are shown in rows E and F of Figure 2. On the terrace there is negligible aldehyde-Cu chemical bonding, such that adsorption is dominated by vdW interactions, so in Table 3 we report distances to the Cu(111) surface plane instead of the closest Cu atom. Aldehydes on the terrace also show negligible preference for any specific orientation or location as long as the molecular plane is nearly parallel to the terrace. On steps, the more reactive step atoms provide more stable and specific adsorption geometries consistent with dative O–Cu bonding. The lowest-energy geometries involve aldehyde O atoms bonded to either a step bridge or to a single step atom, with the rest of the aldehyde suspended over the lower terrace. Formaldehyde is most stable at step atoms and acetaldehyde is most stable at step bridges, but these preferences are weak since the alternate geometry is less stable by at most 0.04 eV. Formaldehyde has an

additional metastable adsorption geometry above a step bridge with its O–C bond directed approximately parallel to the step direction, less stable by only 0.04 eV, suggesting that formaldehyde's potential energy surface is shallower than acetaldehyde's.

Hydrogen

H atoms are most stable at three-fold hollow sites as shown in row G of Figure 2. On the Cu(111) terrace there is a negligible (< 0.01 eV) preference for hcp hollows. The H atom at the hollow site forms three H–Cu bonds of length 1.73 Å. At steps, hydrogen prefers the 3-fold hollow site closest to the step bridge on the upper terrace. This is an fcc hollow site for the (111) step, and an hcp hollow site for the (100) step. The H adsorption geometries have reduced symmetry, forming two H–Cu bonds of length 1.73 Å with the step bridge, and a longer bond of length 1.80 Å with the third Cu atom. Furthermore, while other hollow sites on the upper and lower terraces are metastable, hollow sites at steps are unstable. Top and bridge site geometries are also unstable. Using a clean slab and half the energy of a gas phase H_2 molecule as a reference, hydrogen adsorption energies are -0.28 eV on the terrace, -0.30 eV at the (111) step, and -0.32 eV on the (100) step. H atoms therefore have no significant preference for step edges relative to the Cu(111) terrace.

Coverage

To understand the effect of coverage on stability, we calculated the adsorption energies of ethanol and ethoxy in 4×4 Cu(111) unit cells and unit cells that include 4-atom-wide step edges. For the steps, stability is insensitive to coverage since the change in adsorption energy is negligible (≤ 0.02 eV). For the Cu(111) terrace, however, decreasing coverage increases stability. Ethanol is more stable by 0.06 eV and ethoxy is more stable by 0.04 eV in the 4×4 unit cell than in the 3×3 unit cell. Although hydrogen bonding interactions lead to clustering between adjacent alcohols, intermediate-range alcohol-alcohol interactions are weakly repulsive.[26]

Ethanol Hydrogen Bonding

Alcohols in the gas phase exhibit significant hydrogen bonds with binding energies of up to 0.25 eV.[24] Hydrogen bonding to other alcohols and water can change their adsorption and reactivity on transition metal surfaces such as Cu[11,12] and Rh.[25] In particular, alcohol dehydrogenation on Cu surfaces can be co-catalyzed by water-alcohol hydrogen bonding. To investigate the potential for hydrogen bonding to influence reactivity, we calculate the energy of the hydrogen-bonded dimers relative to the isolated adsorbates:

$$E_{\mathrm{Hbond}} = (E\,[\mathrm{dimer}/X] + E\,[X]) - (E\,[\mathrm{donor}/X] + E\,[\mathrm{acceptor}/X]) \tag{2}$$

where $E\,[A/X]$ is the energy of adsorbate or dimer A on surface X. Negative values indicate that the hydrogen-bonded dimer is more stable than the isolated adsorbates.

Table 4: Hydrogen Bond Energy $E_{\mathbf{Hbond}}$, Donor-Acceptor H$\cdots$O distance $d_{\mathbf{H\cdots O}}$, Donor-Acceptor O–O Distance $d_{\mathbf{O–O}}$, Donor O–Cu Distance $d_{\mathbf{O–Cu}}$, and Acceptor O–Cu Distance $d'_{\mathbf{O–Cu}}$ for Hydrogen Bonding Geometries

Acceptor[a]	Location	E_{Hbond}(eV)	$d_{\mathrm{H\cdots O}}$(Å)	$d_{\mathrm{O–O}}$(Å)	$d_{\mathrm{O–Cu}}$(Å)	$d'_{\mathrm{O–Cu}}$(Å)
EtOH	gas phase	−0.25	1.87	2.84		
	terrace	−0.28	1.64	2.65	2.13	3.13
	(111) step	−0.09	1.63	2.64	2.03	3.56
	(100) step	−0.12	1.74	2.68	2.07	2.43
EtO	gas phase	−0.48	1.45	2.49		
	terrace	−0.06	1.65	2.65	2.17	2.05, 2.10
	(111) step	0.02	1.34	2.43	1.96	1.91
	(100) step	0.05	1.39	2.44	1.97	1.91

[a]The donor is ethanol in all cases.

Although EtOH–EtOH hydrogen bond energies are similar between the gas phase and Cu(111) terrace, hydrogen bonding is much weaker at step sites (see Table 4). This is a consequence of two types of geometric frustration. First, the distance between adjacent step atoms, 2.51 Å is incompatible with the gas phase O$\cdots$O distance of 2.84 Å, as shown in Figure 3. The stronger bonding of step sites to ethanol increases the degree of frustration, weakening hydrogen bonds relative to the terrace and gas phase. Second, alcohol monomers

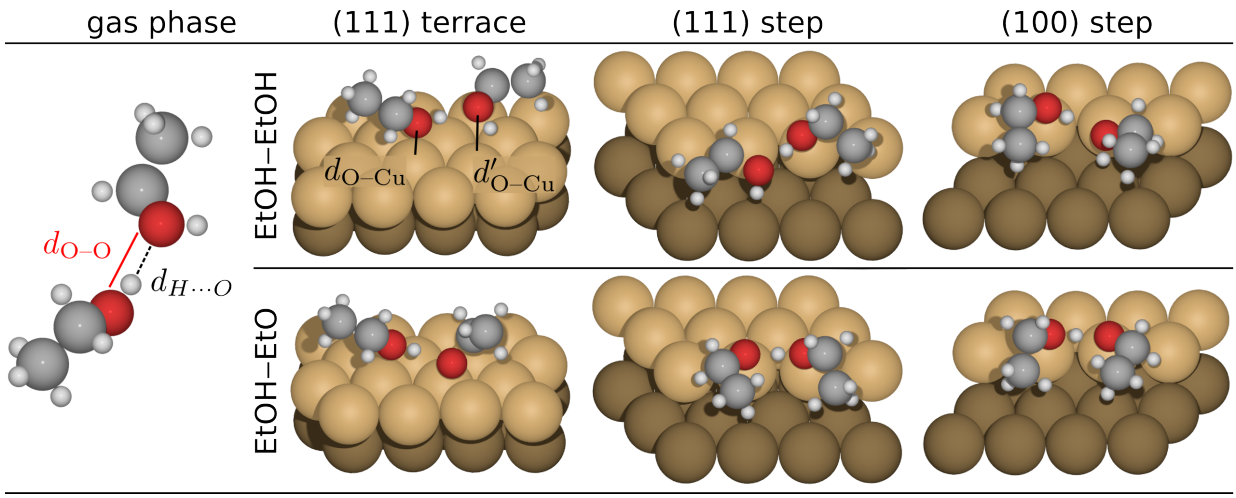

Figure 3: Minimum energy hydrogen-bonded geometries for EtOH–EtOH and EtOH–EtO dimers on each surface. Corresponding energies and geometry values are presented in Table 4.

feature O–H bonds nearly perpendicular to the step direction, at angles of 82° for the (111) step and 74° for the (100) step, but ethanol molecules identically adsorbed at adjacent step atoms would require a donor O–H bond parallel to the step direction instead. This mismatch in distance and O–H orientation destabilizes the EtOH–EtOH dimer relative to isolated ethanol monomers. The resulting step geometries favor hydrogen bonding: the acceptor ethanol's O–Cu bond is significantly lengthened on the (100) step, and broken altogether on the (111) step and terrace.

As in the EtOH–EtOH case, EtOH–EtO hydrogen bonding is stronger in the gas phase and on the terrace than on steps (see Table 4). In the gas phase, EtOH–EtO dimers are strongly bound due to the undercoordinated O atom on the acceptor ethoxy radical, and the hydrogen bond angle is nearly 180°. On the terrace, ethanol prefers top sites while ethoxy prefers fcc hollow sites, but top-hollow site distances are incompatible with the gas phase O$\cdots$O distance of 2.49 Å. Hence, geometric frustration again reduces the binding energy of the dimer. Furthermore, since ethoxy is more strongly bound to the terrace than ethanol, hydrogen bonding is no longer strong enough to cleave all of the ethoxy acceptor O–Cu bonds. The minimum-energy geometry on the terrace partially resolves this geometric frustration by moving the acceptor ethoxy to a bridge site. Step dimers are similarly frustrated. Alcohols

are most stable at step atoms while alkoxys are most stable at step bridges, but no atom-bridge distance matches the gas phase O$\cdots$O distance of 2.49 Å. The resulting geometry is qualitatively different than on the terrace (see Figure 3). Both steps feature EtOH–EtO dimers where the EtOH and EtO fragments form a single O–Cu bond at adjacent top sites. EtOH–EtO dimers at steps are less stable than isolated EtOH and EtO due to significant geometry changes, but the hydrogen bond itself appears to be strong since the hydrogen bond angle and O$\cdots$O distances are very similar to the gas phase values. The donor O–H bond is also longer than in the gas phase, 1.09 Å versus 1.04 Å, while the acceptor H$\cdots$O distance is significantly shorter, 1.38 Å versus 1.65 Å.

Molecular dynamics (MD) simulations of isolated ethanol dehydrogenation intermediates and hydrogen-bonded EtOH–EtOH and EtOH–EtO dimers provide additional insight into hydrogen bonding. Isolated ethanol molecules on the terrace rotate almost freely about the O–Cu bond so O–H bond orientations change approximately every 100 fs. Such frequent rotations suggest a shallow potential energy surface. In contrast, ethanol trajectories on both steps show that the O–H bond is almost always directed toward the lower terrace which suggests a deeper potential energy well. This confirms the assertion made earlier, namely that geometric frustration for the donor ethanol O–H orientation is more significant at step sites. We also confirm that the O–Cu bonds for the accepting ethanol are broken on the terrace and (111) step. On the terrace, the donor ethanol remains adsorbed to the same Cu atom for MD simulation times up to 1 ps while the whole dimer rotates almost freely about the donor O–Cu bond. For the (111) step, the situation is similar where the donor O–H bond shows little energetic preference for a specific angle relative to the step direction over a range of 45°. The behavior at the (100) step is significantly different, as the donor O–H bond does not rotate much and the acceptor ethanol remains bound to a step atom.

For EtOH–EtO dimers we gain similar insights into the bonding from MD simulation trajectories of 1 ps. On all surfaces the EtOH–EtO dimers are metastable and vibrate in place, without any of the nearly free rotations seen for EtOH–EtOH dimers. At both steps the

position of the proton of the H atom relative to the O atoms varies significantly throughout the trajectories. Figure 4(a) shows the superimposed projections of O and proton positions onto u, the O–O axis, and v, the perpendicular direction in the O-O-H plane, relative to the red O atom for each time step. These large variations are the result of the proton "hopping" between the two O atoms approximately every 150 fs as shown in Figure 4(b), precluding clear donor and acceptor assignments. The dynamics are therefore more accurately described as two ethoxy fragments sharing a proton, which remains at least 1.10 Å from either O atom for 90% of the trajectory, indicating strong hydrogen bonding. This direct proton exchange between alcohols and alkoxys could facilitate alcohol-alkoxy displacement reactions reported previously.[23]

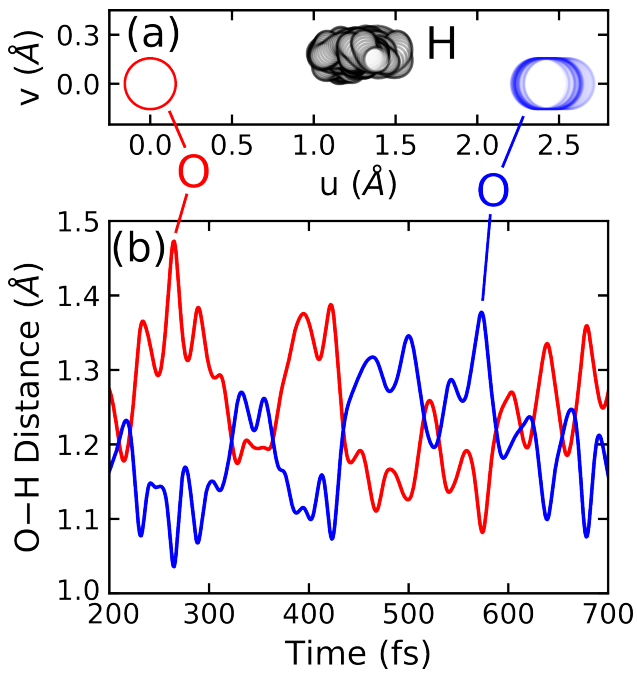

Figure 4: Molecular dynamics results for an EtOH-EtO dimer at the (111) step. (a) Projection of O and proton positions along u, the O-O direction, and v, the perpendicular direction in the O-O-H plane. (b) Distance from the proton to the O atom of the same color in panel (a).

Surface Reactivity

To compare reaction energies and stabilities among different alcohol and surface combinations, we use the DFT total energy of the gas phase alcohol and bare surfaces as a reference. All dehydrogenation intermediates, including H atoms, are considered adsorbed to the same kind of surface. Hydrogen diffusion away from product states is determined using the minimum energies of the isolated hydrogen and adsorbate in separate DFT unit cells

$$\Delta E = E\left[\mathrm{H}/X\right] + E\left[A/X\right] - E_{\mathrm{product}}\left[\left(A + \mathrm{H}\right)/X\right] - E\left[X\right] \tag{3}$$

where A is the intermediate, X is the active site, and E_{product} is the DFT total energy of the nearest local minimum past the transition state. The resulting interaction energies are shown in Figure 5. Since peak aldehyde desorption temperatures are lower than or similar to peak H_2 recombination temperatures in temperature-programmed reaction spectroscopy (TPRS) experiments,[14] we do not include H_2 recombination in Figure 5; energy differences between step types include their relative H atom stabilities. The complete dehydrogenation reaction from gas phase alcohol to gas phase aldehyde and H_2 is significantly endothermic: 0.95 eV for methanol to formaldehyde, and 0.71 eV for ethanol to acetaldehyde. These values are within 0.06 eV of their experimental enthalpies of reaction.[45] Geometries for each of the 12 transition states are shown in Figure 6. Activated C–H bond lengths are significantly longer than activated O–H bond lengths, particularly at step edges, and similar to those found for the Cu(110) surface.[40] These lengths show that transition states for C–H activation are particularly late along the reaction pathway, in agreement with the low ($\leq$ 0.25 eV) activation energies for aldehyde hydrogenation back to alkoxys at steps.

Reaction energy profiles for methanol and ethanol on all three active sites are shown in Figure 5. Steps decrease all activation energies and strengthen all adsorption energies relative to the Cu(111) terrace. The same is true compared to the Cu(110) surface as well,[40] with the exception of C–H bond activation energies which are similar. An important quantity for

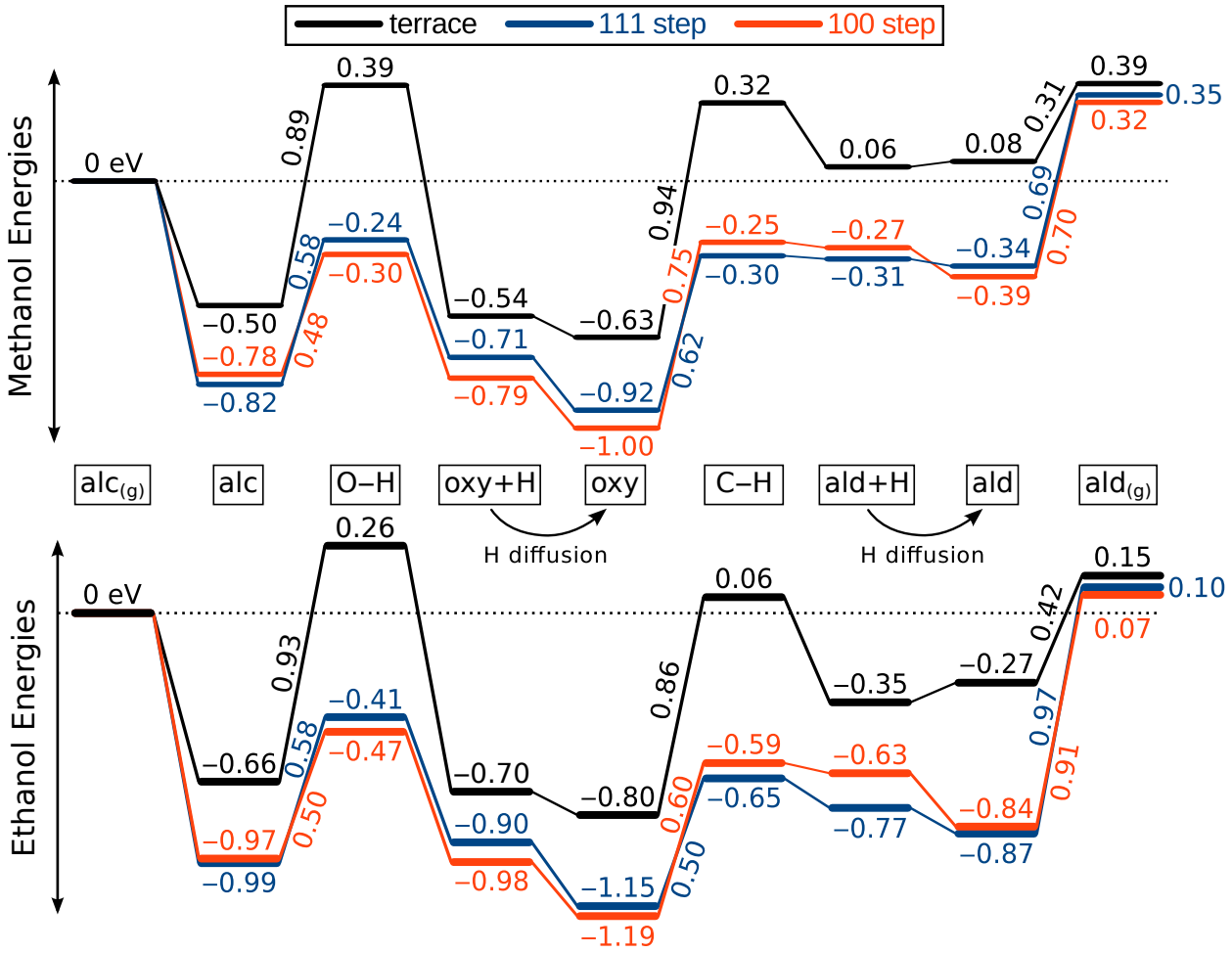

Figure 5: Energies, in eV, for methanol and ethanol dehydrogenation intermediates relative to gas phase alcohols and clean surfaces for the Cu(111) terrace (black), (111) step (blue), and (100) step (red). Steps are labeled as "alc" for alcohols, "oxy" for alkoxys, and "ald" for aldehydes. X+H indicates X coadsorbed with H, and X–H indicates the corresponding transition state. Energies for H_2 desorption are omitted for clarity; values include atomic H adsorption at each surface.

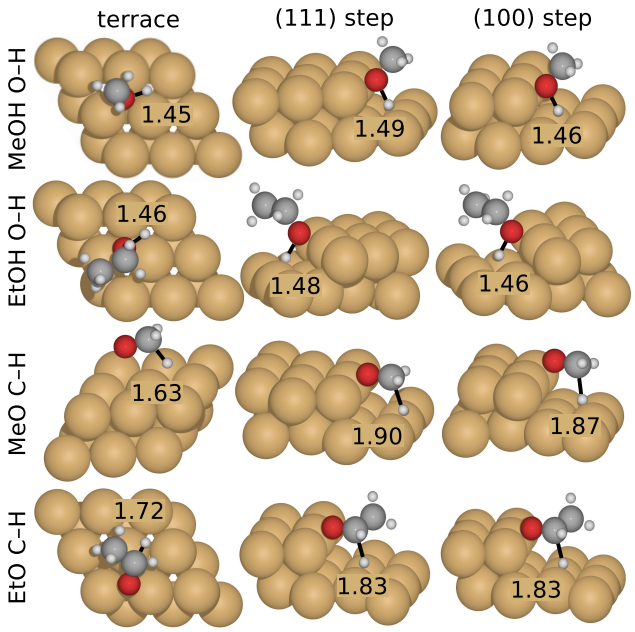

Figure 6: Transition states for O–H and C–H bond activation for the Cu(111) terrace and the (111) and (100) step edges. Numbers indicate the activated bond length in Å.

dehydrogenation activity is the relative probability of desorption versus O–H bond activation, which is exponential in the "branching energy" $\Delta E_A^{\text{O–H}} - \Delta E_{\text{desorb}}$. The branching energy is 0.39 eV for methanol and 0.26 eV for ethanol on the Cu(111) terrace, making desorption much more likely than O–H activation. In contrast, step edges provide significantly higher desorption energies and lower activation energies, yielding a negative branching energy and thus increasing catalytic activity. Steps are therefore predicted to contribute most of the surface reactivity under UHV conditions, in agreement with experimental results.[14]

Another major trend is the difference in stability and reactivity between methanol and ethanol. Ethanol and ethoxy are more stable than methanol and methoxy by about 0.18 eV on all three surfaces, respectively. The difference in adsorption energies between acetaldehyde and formaldehyde is more variable, ranging from 0.11 eV on the terrace to 0.28 eV on the (111) step. There is little difference in O–H activation energies; the methanol and ethanol values are within 5% at each site. In contrast, ethoxy C–H activation energies are all lower than their methoxy counterparts, by about 10% for the terrace and 20% on both steps.

Alcohols to Alkoxys

Steps significantly reduce the activation energy of O–H bond cleavage for both alcohols. Their O–H transition states have the alkoxy fragment adsorbed to a step bridge and a H atom near a three-fold hollow site on the lower terrace. The metastable product state consists of the alkoxy at the step bridge and H at the same 3-fold hollow site on the lower terrace. This state is less stable than having H and the alkoxy on separated slabs, primarily due to the significantly lower stability of H below the step relative to the terrace above the step (by about 0.2 eV).

On the terrace, the O–H bond is cleaved over a bridge site, with the alkoxy and H fragments adsorbed at adjacent hcp and fcc hollow sites, respectively. Isolated alkoxys are more stable by about 0.04 eV at fcc hollow sites but transition states with alkoxys at hcp sites are more stable by $\leq$ 0.03 eV. Following O–H cleavage the alkoxy diffuses across a Cu–Cu bridge to an adjacent fcc site. Alkoxy-H interactions are repulsive on the terrace, possibly due to Coulomb repulsion. Using methanol dehydrogenation as an example, the net Hirshfeld charges on the alcohol O and H atoms start at $q_{\mathrm{O}} = -0.16$ e and $q_{\mathrm{H}} = +0.14$ e, and decrease throughout the reaction to $q_{\mathrm{O}} = -0.22$ e and $q_{\mathrm{H}} = -0.12$ e in the coadsorbed product geometry. Compared to steps, higher Cu atom coordination and weaker alkoxy adsorption destabilize the transition state on the Cu(111) terrace.

Given that previous work[11] found that water-methanol hydrogen bonding facilitates alcohol dehydrogenation on Cu(111) surfaces, we consider the possibility that ethanol-ethanol might also facilitate dehydrogenation. Alcohol dehydrogenation for EtOH–EtOH dimers takes place through a coordinated two-proton mechanism, regardless of which alcohol bond is pre-stretched for the dimer method: the donor ethanol loses its proton to the acceptor ethanol, while the acceptor ethanol loses its proton to the Cu(111) surface. The activation energy for this process is 0.89 eV, only slightly less than the activation energy for an isolated ethanol molecule, and still significantly higher than the ethanol desorption energy of 0.66 eV from the Cu(111) surface. Therefore ethanol-ethanol hydrogen bonding is not predicted to

facilitate anhydrous dehydrogenation on atomically flat Cu(111) surfaces in agreement with experimental results with high initial ethanol coverage.[14]

Alkoxys to Aldehydes

Like O–H bond activation, C–H bond activation proceeds differently on step sites than on the Cu(111) terrace. To cleave the C–H bond on the terrace, the alkoxy O–C bond first tilts toward the surface to reduce the distance between the H atom and the terrace, followed by H abstraction to a fcc hollow site. The C–H activation energy is lower for ethoxy than for methoxy. In addition, C–H cleavage is significantly endothermic for both alkoxys so the activation energies for hydrogenation back to the alkoxy are 0.26 eV for formaldehyde and 0.41 eV for acetaldehyde.

Reactions at steps have significantly lower activation energies than on the terrace, a result of favorable alkoxy adsorption geometries. First, alkoxys already have O–C bonds approximately parallel to the terrace so the abstracted H atom starts approximately 0.5 Å closer to the Cu surface than on the flat Cu(111) terrace. Second, minimum-energy aldehyde geometries have similar O–C and C–C orientations relative to the step edge, reducing the amount of molecular distortion and hence the activation energy required to reach the transition state.

Alkoxys and aldehydes are both more stable at steps so the net reaction energies are approximately as endothermic as on the terrace. Combined with the lower transition state energy, at steps C–H bond formation has very low activation energy. The largest such activation energy is only 0.25 eV so aldehyde hydrogenation should occur readily at the desorption temperatures of 300-400 K for aldehydes reported in experiments.[14]

Aldehyde Desorption

We find that aldehyde desorption from Cu(111) step sites is strongly affected by kinetic competition. Aldehyde desorption temperatures are significantly higher in temperature-

programmed reaction spectroscopy (TPRS) experiments, in which the alcohol is dosed, than in temperature-programmed desorption (TPD) experiments, in which the aldehyde itself is dosed. However, Figure 5 shows that alkoxy C–H bond activation is not the rate-limiting step. Using simple kinetic arguments similar to previous work,[46] we show that kinetic competition between reversible hydrogenation and irreversible desorption significantly increases the effective aldehyde desorption energy in TPRS experiments compared to TPD experiments.

Reversible aldehyde hydrogenation and irreversible desorption can be described using simple first and second-order rate expressions. We consider the rates of alkoxy dehydrogenation k_f, aldehyde hydrogenation k_r, and aldehyde desorption k_d per lattice site:

$$k_f = A_f\, \theta_{\mathrm{alk}}\, (1 - \Theta_{\mathrm{T}})\, e^{-\beta \Delta E_A^f} \tag{4}$$

$$k_r = A_r\, \theta_{\mathrm{ald}}\, \theta_{\mathrm{H}}\, e^{-\beta \Delta E_A^r} \tag{5}$$

$$k_d = A_d\, \theta_{\mathrm{ald}}\, e^{-\beta E_{\mathrm{ads}}} \tag{6}$$

$$\theta_o = \theta_{\mathrm{alk}} + \theta_{\mathrm{ald}} \tag{7}$$

where θ_X values are coverages, $\theta_o \sim 10\%$ is the coverage of active sites,[14] Θ_{T} is the total coverage on the terrace, and the prefactors $A_f = 10^{13}$ Hz, $A_r = 2 \times 10^{12}$ Hz, and $A_d = 10^{15.5}$ Hz are typical values for first-order reactions, second-order reactions, and first-order desorption,[47] respectively. Hydrogen recombines at higher temperatures than aldehyde desorption[14] so H atoms are kinetically trapped and thus $\theta_{\mathrm{H}} = \theta_{\mathrm{alk}} + 2\theta_{\mathrm{ald}} \geq \theta_o$. Moreover, all adsorbates except H are significantly more stable at steps so $\Theta_{\mathrm{T}} \approx \theta_{\mathrm{H}}$. Aldehyde hydrogenation barriers are much lower than their desorption energies at steps, so even the lower bound $\theta_{\mathrm{H}} = \theta_o$ gives $(k_r/k_d) \geq 2.4 \times 10^5$ at 300 K. The vastly higher hydrogenation rate yields an equilibrium between aldehyde hydrogenation and alkoxy dehydrogenation.

Equilibrium gives a fully-determined system of equations. Defining $B \equiv e^{-\beta\left(\Delta E_A^f - \Delta E_A^r\right)}$, where $B \leq 2.0 \times 10^{-5}$ at 300 K, we obtain the following important results to first order in

B:

$$\frac{\theta_{\text{ald}}}{\theta_{\text{alk}}} \approx \frac{1-\theta_o}{\theta_o}\frac{A_f}{A_r}B \tag{8}$$

$$k_d \approx (1-\theta_o)\,A_d\,\frac{A_f}{A_r}\,e^{-\beta\left(E_{\text{ald,(g)}}-E_{\text{alk}}\right)} \tag{9}$$

Equation 8 predicts a formaldehyde to methoxy ratio of approximately 1:(2×10^7), and an acetaldehyde to ethoxy ratio of approximately 1:500 at their peak TPRS desorption temperatures of 370 and 320, respectively. Alkoxys are predicted to be the majority species in all cases. Expressing k_d in terms of the dominant alkoxy coverage, $\theta_{\text{ald}} \approx \theta_o$, results in eq 9, showing the effective aldehyde desorption is the total energy difference between the gas phase aldehyde and the adsorbed alkoxy. Alkoxys are significantly more stable than their corresponding aldehydes so kinetic competition increases the effective aldehyde desorption temperature. These predictions are in excellent agreement with the observed TPRS temperatures as discussed below. The critical factor leading to these results is $(k_r/k_d) \gg 1$, a combination of high aldehyde desorption energy and low activation energy for C–H bond formation at step edges.

Temperature Comparison with Experiments

To check the correspondence between our DFT calculations and recent experimental measurements, we use the Redhead equation for first-order kinetics to calculate peak TPD temperatures $T_{\text{max}}^{\text{DFT}}$ from desorption energies

$$\frac{E_{\text{A}}}{k\,T_{\text{max}}^2} = \frac{v}{r}\exp\left(\frac{E_a}{k\,T_{\text{max}}}\right) \tag{10}$$

where $r = 1.0$ K/s is the heating rate, k is the Boltzmann constant, and $v = 10^{15.5}$ Hz is a typical desorption prefactor for adsorbates like CO and methanol.[47] We compare to the experimental data of Wang et al.,[14] who report desorption temperatures for flat and stepped

Cu(111) surfaces dosed with methanol, ethanol and acetaldehyde, as well as the reaction rate limited desorption temperatures of formaldehyde and acetaldehyde. The same experimental temperature is assigned to both step edges, and the activation energy for reaction rate-limited aldehyde desorption is assumed to be the total energy difference between adsorbed alkoxys and their gas phase aldehydes as discussed previously. As shown in Figure 7 with dark circles, the DFT calculations and chosen prefactor typically overestimate desorption temperatures by about 41 K. The linear correlation suggests that DFT calculations are reliable for obtaining catalytic trends. Furthermore, we extrapolate our ethanol results with the trend of 0.18 eV/CH_2 to predict experimental TPD temperatures for isopropanol and acetone[48] desorption, as well as 1-butanol, butyraldehyde, crotyl alcohol, and crotanaldehyde.[49] For these predictions we use the Redhead equation as above with the experimental heating rates. These predictions, shown in Figure 7 as open squares, follow a similar trend to the fitted line which suggests that the 0.18 eV/CH_2 PBE+vdW trend generalizes well to longer alcohols.

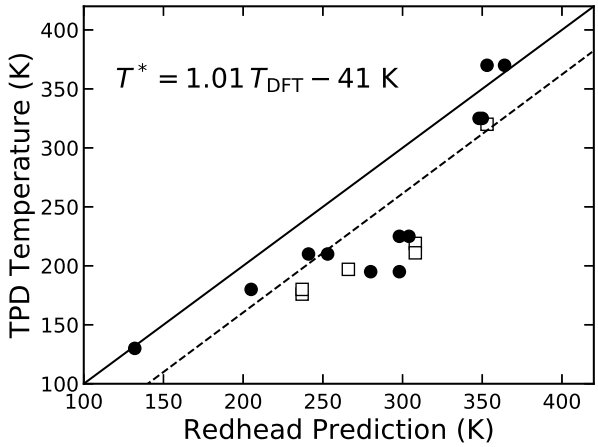

Figure 7: Parity plot of experimental TPD temperatures versus DFT predictions via the Redhead equation (see text). Solid line: 1:1 parity. Dashed line: fit to methanol and ethanol results (dark circles). Open squares compare extrapolated desorption temperatures for isopropanol, 1-butanol, crotyl alcohol, and their aldehydes with experimental TPD values.

Implications for Reactivity

Branching Energies for Longer Alcohols

Since O–H activation energies are very similar between methanol and ethanol, we expect them to be similar for longer alcohols as well. The limiting factor for UHV methanol and ethanol dehydrogenation on Cu(111) single crystals is their high branching energies. If each additional CH_2 subunit contributes a similar adsorption energy change of 0.18 eV without changing the O–H activation energy, then longer alcohols will increasingly favor reaction over desorption. A similar increase in reactivity is predicted for longer alcohols on the Cu(110) surface.[40] The ethanol branching energy, the difference between its O–H activation energy and desorption energy, is 0.27 eV on the terrace so desorption is strongly favored over reaction. However, with the trend of 0.18 eV/CH_2, longer alcohols will have increasingly favorable branching energies. For example, n-propanol should have a lower branching energy of approximately 0.09 eV and n-butanol should have a branching energy of approximately −0.09 eV. We therefore hypothesize that Cu(111) terraces can selectively dehydrogenate longer alcohols starting with n-butanol.

Competitive Binding

Despite a higher calculated O–H activation energy, our previous investigation of isolated Pt atoms in Cu(111) single crystal surfaces[14] (single-atom alloys) found greater catalytic activity than steps for alcohol dehydrogenation. We believe this is the result of "self-poisoning" at steps where alkoxy products favorably compete with alcohol reactants for adsorption. On the Pt-Cu(111) surface, ethoxy-Pt interactions are repulsive and ethoxy groups adjacent to the Pt active site are less stable than at longer distances. In contrast, in this study steps are the most stable binding sites for alkoxys. To achieve catalytic turnover at steps, alkoxy products must diffuse away from step edges to make way for additional alcohol adsorption. This is likely to slow down dehydrogenation kinetics at high alkoxy coverages. Furthermore, alkoxy-

alcohol replacement is slightly endothermic for ethanol at both steps and for methanol at the (100) step (by < 0.1 eV), effectively increasing the activation energy for subsequent O–H bond breaking. Making alkoxy adsorption weaker or altogether unstable could mitigate these kinetic and thermodynamic limitations. We therefore hypothesize that catalytic turnover for O–H activation could be improved if step edges were chemically modified to destabilize alkoxy adsorption. At high hydrogen coverage such modifications would also reduce aldehyde desorption temperatures since they are dictated by alkoxy stability as well.

Hydrogen Recombination

In addition to destabilizing alkoxy adsorption, another way to reduce aldehyde desorption temperatures is to reduce hydrogen coverage. Alkoxys adsorb more strongly than their corresponding aldehydes, so reversible aldehyde hydrogenation to the alkoxy increases aldehyde desorption temperatures. Hydrogen desorbs from the Cu(111) terrace near 370 K at low coverages, a temperature similar to or higher than aldehyde desorption temperatures, so H coverage is expected to be high in TPRS experiments. The activation energy for hydrogen recombination can be reduced by introducing other active sites on the surface. For example, isolated Pt atoms in the Cu(111) surface layer reduce the H_2 recombination temperature to approximately 255 K in TPD experiments for anhydrous ethanol dehydrogenation.[14] Reduced hydrogen coverage would limit aldehyde hydrogenation back to alkoxys and therefore reduce the peak TPRS temperature for aldehyde desorption.

Conclusions

In this work we investigated anhydrous alcohol dehydrogenation on the Cu(111) surface and its steps. The presence of steps increases adsorption energies for all intermediates. Including vdW corrections further increases adsorption energies by more than 50% in all cases and favors shorter adsorbate-Cu distances. ZPE corrections yield a minor ($< 10\%$)

effect on adsorption, but a significant reduction in O–H and C–H bond activation energies by ~ 0.21 eV. Finally, while hydrogen bonds are significant in the gas phase and on the terrace, geometric frustration limits their stability at step edges. EtOH–EtO dimers at step edges are less stable than isolated EtOH and EtO, but still exhibit strong H-bonding characteristics and a "proton hopping" mechanism with significant variations in O–H distances.

Steps also significantly improve reactivity by reducing O–H and C–H activation energies to values lower than alcohol desorption energies. With O–H bond activation energies lower than desorption energies, steps will be highly reactive, while the opposite is found for the Cu(111) terrace. Step edges on Cu(111) are also predicted to be somewhat more reactive overall for anhydrous alcohol dehydrogenation than clean Cu(110) surfaces. Furthermore, the low C–H bond activation energies makes alkoxy dehydrogenation highly reversible. Acetaldehyde desorption from steps is therefore predicted to be limited due to kinetic competition so desorption temperatures are dictated by the greater alkoxy stability. Peak TPD and TPRS temperatures calculated at step edges using DFT based on this prediction are in good agreement with experimental results for methanol, ethanol, and acetaldehyde desorption from Cu(111). In contrast, kinetic competition does not take place on the Cu(111) terrace due to the higher C–H activation energies and lower aldehyde desorption energies.

In light of these results we propose three directions for further work on alcohol dehydrogenation on Cu(111) surfaces: (i) The additional CH_2 subunit of ethanol increases its desorption energy by 0.18 eV relative to methanol while preserving the O–H activation energy. If this trend continues to larger alcohols, desorption energies are predicted to exceed O–H activation energies on the Cu(111) terrace starting with n-butanol and thus lead to length-selective alcohol dehydrogenation. (ii) Alcohols and alkoxys are similarly stable at step edges so catalytic turnover is limited. Alkoxy binding could be destabilized by doping, facilitating their replacement with unreacted alcohols to improve catalytic turnover and UHV aldehyde yield. (iii) Aldehyde desorption temperatures are increased in the presence of coadsorbed H due to reversible aldehyde hydrogenation. If surfaces were chemically modified

to facilitate H_2 desorption at lower temperatures, the resulting decrease in H coverage would limit C–H hydrogenation rates and lead to aldehyde desorption at lower temperatures in TPRS experiments.

Acknowledgement

We thank Professor Robert J. Madix for his constructive feedback. This work was supported by Integrated Mesoscale Architectures for Sustainable Catalysis, an Energy Frontiers Research Center funded by the U.S. Department of Energy, Office of Science, Basic Energy Sciences under Award DE-SC0012573. Calculations were performed using resources supported by the U.S. Department of Energy, Office of Science: the Oak Ridge National Leadership Computing Facility at Oak Ridge National Laboratory, under Contract No. DE-AC05-00OR22725, and the National Energy Research Scientific Computing Center, a DOE Office of Science User Facility under Contract No. DE-AC02-05CH11231. Additional calculations were run on the Odyssey cluster supported by the FAS Division of Science, Research Computing Group at Harvard University.

References

(1) Su, S.; Zaza, P.; Renken, A. Catalytic Dehydrogenation of Methanol to Water-Free Formaldehyde. *Chem. Eng. Technol.* **1994**, *17*, 34–40.

(2) Franz, A. W.; Kronemayer, H.; Pfeiffer, D.; Pilz, R. D.; Reuss, G.; Disteldorf, W.; Gamer, A. O.; Hilt, A. Formaldehyde. 2016.

(3) Gerberich, H. R.; Seaman, G. C. *Kirk-Othmer Encycl. Chem. Technol.*; John Wiley & Sons, Inc.: Hoboken, NJ, USA, 2013.

(4) Žilnik, L. F.; Golob, J. Analysis of Separation of a Water-Methanol-Formaldehyde Mixture. *Acta Chim. Slov.* **2003**, *50*, 451–460.

(5) Bowker, M.; Madix, R. J. XPS, UPS and Thermal Desorption Studies of Alcohol Adsorption on Cu(110): I. Methanol. *Surf. Sci.* **1980**, *95*, 190–206.

(6) Russell, J.; Gates, S.; Yates, J. Reaction of Methanol with Cu(111) and Cu(111) + O(ads). *Surf. Sci.* **1985**, *163*, 516–540.

(7) Johnston, S. M.; Mulligan, A.; Dhanak, V.; Kadodwala, M. The Structure of Methanol and Methoxy on Cu(111). *Surf. Sci.* **2003**, *530*, 111–119.

(8) Hofmann, P.; Schindler, K.-M.; Bao, S.; Fritzsche, V.; Ricken, D.; Bradshaw, A.; Woodruff, D. The Geometric Structure of the Surface Methoxy Species on Cu(111). *Surf. Sci.* **1994**, *304*, 74–84.

(9) Chen, A.; Masel, R. Direct Conversion of Methanol to Formaldehyde in the Absence of Oxygen on Cu(210). *Surf. Sci.* **1995**, *343*, 17–23.

(10) Bowker, M.; Madix, R. XPS, UPS and Thermal Desorption Studies of Alcohol Adsorption on Cu(110): II. Higher Alcohols. *Surf. Sci.* **1982**, *116*, 549–572.

(11) Boucher, M. B.; Marcinkowski, M. D.; Liriano, M. L.; Murphy, C. J.; Lewis, E. A.; Jewell, A. D.; Mattera, M. F. G.; Kyriakou, G.; Flytzani-Stephanopoulos, M.; Sykes, E. C. H. Molecular-Scale Perspective of Water-Catalyzed Methanol Dehydrogenation to Formaldehyde. *ACS Nano* **2013**, *7*, 6181–6187.

(12) Shan, J.; Lucci, F. R.; Liu, J.; El-Soda, M.; Marcinkowski, M. D.; Allard, L. F.; Sykes, E. C. H.; Flytzani-Stephanopoulos, M. Water Co-Catalyzed Selective Dehydrogenation of Methanol to Formaldehyde and Hydrogen. *Surf. Sci.* **2016**, *650*, 121–129.

(13) Wang, Z. T.; Hoyt, R. A.; El-Soda, M.; Madix, R. J.; Kaxiras, E.; Sykes, E. C. H. Dry Dehydrogenation of Ethanol on Pt-Cu Single Atom Alloys. *Top. Catal.* **2017**, 1–8.

(14) Wang, Z.-T.; Xu, Y.; El-Soda, M.; Lucci, F. R.; Madix, R. J.; Friend, C. M.; Sykes, E.

C. H. Surface Structure Dependence of the Dry Dehydrogenation of Alcohols on Cu(111) and Cu(110). *J. Phys. Chem. C* **2017**, *121*, 12800–12806.

(15) Greeley, J.; Mavrikakis, M. Methanol Decomposition on Cu(111): A DFT Study. *J. Catal.* **2002**, *208*, 291–300.

(16) Gomes, J. R. B.; Gomes, J. A. N. F. A DFT Study of the Methanol Oxidation Catalyzed by a Copper Surface. *Surf. Sci.* **2001**, *471*, 59–70.

(17) Behrens, M.; Studt, F.; Kasatkin, I.; Kühl, S.; Hävecker, M.; Abild-Pedersen, F.; Zander, S.; Girgsdies, F.; Kurr, P.; Kniep, B.-L. et al. The Active Site of Methanol Synthesis over Cu/ZnO/Al2O3 Industrial Catalysts. *Science* **2012**, *336*, 893–897.

(18) Studt, F.; Abild-Pedersen, F.; Varley, J. B.; Nørskov, J. K. CO and CO2 Hydrogenation to Methanol Calculated Using the BEEF-vdW Functional. *Catal. Letters* **2013**, *143*, 71–73.

(19) Li, X.; Lim, K. H. DFT Study of Steam Reforming of Formaldehyde on Cu, PdZn, and Ir. *ChemCatChem* **2012**, *4*, 1311–1320.

(20) Li, R.; Zhang, M.; Yu, Y. A DFT Study on the Cu (111) Surface for Ethyl Acetate Synthesis from Ethanol Dehydrogenation. *Appl. Surf. Sci.* **2012**, *258*, 6777–6784.

(21) Tereshchuk, P.; Da Silva, J. L. F. Ethanol and Water Adsorption on Close-Packed 3d, 4d, and 5d Transition-Metal Surfaces: A Density Functional Theory Investigation with van der Waals Correction. *J. Phys. Chem. C* **2012**, *116*, 24695–24705.

(22) Zhang, R.; Wang, G.; Wang, B. Insights Into the Mechanism of Ethanol Formation from Syngas on Cu and an Expanded Prediction of Improved Cu-Based Catalyst. *J. Catal.* **2013**, *305*, 238–255.

(23) Karakalos, S.; Xu, Y.; Cheenicode Kabeer, F.; Chen, W.; Rodríguez-Reyes, J. C. F.; Tkatchenko, A.; Kaxiras, E.; Madix, R. J.; Friend, C. M. Noncovalent Bonding Controls

Selectivity in Heterogeneous Catalysis: Coupling Reactions on Gold. *J. Am. Chem. Soc.* **2016**, *138*, 15243–15250.

(24) Fileti, E. E.; Chaudhuri, P.; Canuto, S. Relative Strength of Hydrogen Bond Interaction in Alcohol-Water Complexes. *Chem. Phys. Lett.* **2004**, *400*, 494–499.

(25) Michel, C.; Auneau, F.; Delbecq, F.; Sautet, P. C-H versus O-H Bond Dissociation for Alcohols on a Rh(111) Surface: A Strong Assistance from Hydrogen Bonded Neighbors. *ACS Catal.* **2011**, *1*, 1430–1440.

(26) Lawton, T. J.; Carrasco, J.; Baber, A. E.; Michaelides, A.; Sykes, E. C. H. Hydrogen-Bonded Assembly of Methanol on Cu(111). *Phys. Chem. Chem. Phys.* **2012**, *14*, 11846.

(27) Kresse, G.; Hafner, J. Ab Initio Molecular Dynamics for Liquid Metals. *Phys. Rev. B* **1993**, *47*, 558–561.

(28) Kresse, G.; Hafner, J. Ab Initio Molecular-Dynamics Simulation of the Liquid-Metal-Amorphous-Semiconductor Transition in Germanium. *Phys. Rev. B* **1994**, *49*, 14251–14269.

(29) Kresse, G.; Furthmüller, J. Efficiency of Ab Initio Total Energy Calculations for Metals and Semiconductors Using a Plane-Wave Basis Set. *Comput. Mater. Sci.* **1996**, *6*, 15–50.

(30) Kresse, G.; Furthmüller, J. Efficient Iterative Schemes for Ab Initio Total-Energy Calculations Using a Plane-Wave Basis Set. *Phys. Rev. B* **1996**, *54*, 11169–11186.

(31) Perdew, J. P.; Burke, K.; Ernzerhof, M. Generalized gradient approximation made simple. *Phys. Rev. Lett.* **1996**, *77*, 3865–3868.

(32) Perdew, J. P.; Burke, K.; Ernzerhof, M. Erratum: Generalized Gradient Approximation Made Simple. *Phys. Rev. Lett.* **1997**, *78*, 1396.

(33) Bitzek, E.; Koskinen, P.; Gähler, F.; Moseler, M.; Gumbsch, P. Structural Relaxation Made Simple. *Phys. Rev. Lett.* **2006**, *97*, 170201.

(34) Pack, J. D.; Monkhorst, H. J. Special Points for Brillouin-Zone Integrations. *Phys. Rev. B* **1976**, *13*, 5188–5192.

(35) Tkatchenko, A.; Scheffler, M. Accurate Molecular van der Waals Interactions from Ground-State Electron Density and Free-Atom Reference Data. *Phys. Rev. Lett.* **2009**, *102*, 073005.

(36) Henkelman, G.; Jónsson, H. A Dimer Method for Finding Saddle Points on High Dimensional Potential Surfaces Using Only First Derivatives. *J. Chem. Phys.* **1999**, *111*, 7010–7022.

(37) Heyden, A.; Bell, A. T.; Keil, F. J. Efficient Methods for Finding Transition States in Chemical Reactions: Comparison of Improved Dimer Method and Partitioned Rational Function Optimization method. *J. Chem. Phys.* **2005**, *123*, 224101.

(38) Heid, R.; Bohnen, K. P.; Kara, A.; Rahman, T. S. Ab initio calculations of multilayer relaxations of stepped Cu surfaces. *Phys. Rev. B - Condens. Matter Mater. Phys.* **2002**, *65*, 1–8.

(39) Grimme, S.; Antony, J.; Ehrlich, S.; Krieg, H. A Consistent and Accurate Ab Initio Parametrization of Density Functional Dispersion Correction (DFT-D) for the 94 Elements H-Pu. *J. Chem. Phys.* **2010**, *132*, 154104.

(40) Chen, W.; Cubuk, E. D.; Montemore, M. M.; Reece, C.; Madix, R. J.; Friend, C. M.; Kaxiras, E. A Comparative Ab Initio Study of Anhydrous Dehydrogenation of Linear-Chain Alcohols on Cu(110). *J. Phys. Chem. C* **2018**, acs.jpcc.8b01698.

(41) Gomes, J. R. B.; Gomes, J. A. N. F.; Illas, F. First-Principles Study of the Adsorption

of Formaldehyde on the Clean and Atomic Oxygen Covered Cu(111) surface. *J. Mol. Catal. A Chem.* **2001**, *170*, 187–193.

(42) Zhang, M.; Yao, R.; Jiang, H.; Li, G.; Chen, Y. Catalytic Activity of Transition Metal Doped Cu(111) Surfaces for Ethanol Synthesis from Acetic Acid Hydrogenation: a DFT Study. *RSC Adv.* **2017**, *7*, 1443–1452.

(43) Csonka, G. I.; Perdew, J. P.; Ruzsinszky, A.; Philipsen, P. H. T.; Lebègue, S.; Paier, J.; Vydrov, O. A.; Ángyán, J. G. Assessing the Performance of Recent Density Functionals for Bulk Solids. *Phys. Rev. B* **2009**, *79*, 155107.

(44) Narasimhan, S.; de Gironcoli, S. Ab Initio Calculation of the Thermal Properties of Cu: Performance of the LDA and GGA. *Phys. Rev. B* **2002**, *65*, 064302.

(45) Afeefy, H. Y.; Liebman, J. F.; Stein, S. E. In *NIST Chemistry WebBook, NIST Standard Reference Database Number 69*; Linstrom, P. J., Mallard, W. G., Eds.; National Institute of Standards and Technology: Gaithersburg, MD, 2018.

(46) Michel, C.; Zaffran, J.; Ruppert, A. M.; Matras-Michalska, J.; Jędrzejczyk, M.; Grams, J.; Sautet, P. Role of Water in Metal Catalyst Performance for Ketone Hydrogenation: a Joint Experimental and Theoretical Study on Levulinic Acid Conversion into Gamma-Valerolactone. *Chem. Commun.* **2014**, *50*, 12450–12453.

(47) Campbell, C. T.; Árnadóttir, L.; Sellers, J. R. V. Kinetic Prefactors of Reactions on Solid Surfaces. *Zeitschrift für Phys. Chemie* **2013**, *227*, 1435–1454.

(48) Miller, B. P.; Furlong, O. J.; Tysoe, W. T. Surface Chemistry of Isopropoxy Tetramethyl Dioxaborolane on Cu(111). *Langmuir* **2012**, *28*, 6322–6327.

(49) Mulligan, A.; Kadodwala, M. Destabilizing Effects of Thiols on Bonding to a Noble Metal: The Effects of Methanethiolate on the Bonding of Aldehydes and Alcohols on Cu(111). *J. Phys. Chem. C* **2010**, *114*, 21457–21464.
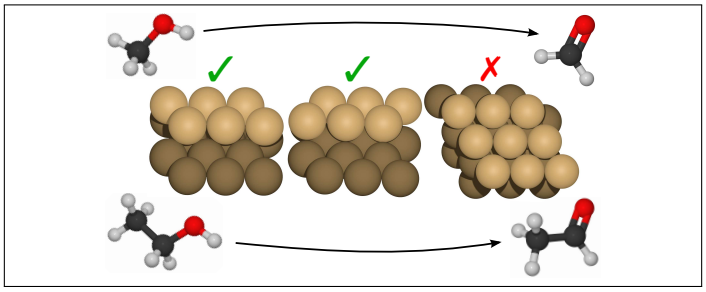
Graphical TOC Entry